BRIGHTNESS TEMPERATURE OF DECAMETER SOLAR BURSTS WITH HIGH-FREQUENCY CUT-OFF

A. A. Stanislavsky*, A. A. Konovalenko*, Ya. S. Volvach*, and A. A. Koval*†

Abstract

In this paper we consider solar bursts with a high-frequency cut-off, simultaneously observed by several ground-based radio observatories located at significant distances from each other. The events were correlated with the emergence of a new group of solar spots on the far side of the Sun. The cut-off effect of the solar bursts was caused by the occultation of their radiating sources by the solar corona for observers on Earth. Based on the radio occultation of the low-frequency burst sources in the solar corona, we have estimated their angular sizes. This makes it possible to obtain the dynamic spectra of the solar bursts in terms of brightness temperature.

1 Introduction

Usually, the sources of solar radio bursts are spatially resolved with interferometers and heliographs. The observations show that the typical size of burst sources increases with wavelength growth. Type II and IV bursts at meter wavelength often have irregular shape and sometimes exceed the size of the visual solar disk, whereas the type I and III bursts are simpler and smaller. However, our knowledge about source sizes of solar bursts at low frequencies is greatly limited. Therefore, one of the challenges for modern low-frequency radio astronomy arrays (LOFAR, GURT, LWA, MWA, NenuFAR and SKA) is to provide the study of the image of solar burst sources and their angular sizes. The variety of such bursts and their fine frequency–time structure continually amaze. In addition to conventional bursts of II, III and IV types many other radio events are detected (striae, drift pairs, S-bursts and so on). Each of them has its own radio emission mechanism and a source size characteristic for it. This work attempts to fill the gap in our knowledge about low-frequency burst source sizes by an original method. Its essence consists of

* *Institute of Radio Astronomy, National Academy of Sciences of Ukraine, Kharkiv, Ukraine*
† *Institute of Space Sciences and School of Space Science and Physics, Shandong University, Weihai, China*

the following. Flares that are partially occulted by the solar limb provide not only the most hopeful source of information about hard X-ray loop–top sources, but due to CMEs the accompanied behind–limb bursts become available for the study of their source size features. Our analysis is devoted to such events.

The principal aim of this study is to estimate angular sizes and brightness temperatures of their sources. The brightness temperature is an important indicator of observed emission, distinguishing emission processes between thermal, non-thermal incoherent and coherent. For solar radio sources, the high brightness temperatures imply a form of coherent emission, an example of which is the plasma emission responsible for the type III bursts from the solar corona.

In this paper we present the results of observations of several tens of solar behind–limb burst events at 9–33 MHz. The bursts were recorded with the Ukrainian decameter radio telescope, UTR-2 (near Kharkiv, Ukraine) on 17–19 August of 2012. We also discuss features of such bursts and consider the associated radio and plasma phenomena observed simultaneously by STEREO, GOES and SOHO spacecraft.

2 Solar events and observational facilities

The main peculiarity of solar activity on 17–19 August 2012 was the emergence of a new group of solar spots (AR 11548 with N19E87) on the far side (generating many moderate flares over the eastern limb) of the Sun. Moreover, the solar activity was also accompanied by many coronal mass ejections (CMEs) and radio bursts, shown in Table 1. The radio bursts were mainly related to type III and IIIb–III bursts, but some of them had unusual high-frequency cut-off features to which we will pay much attention below.

During this observation the UTR-2 radio telescope was operated in the mode using four sections of the north–south array of the antenna [Braude et al., 1978; Konovalenko et al., 2016]. Recall, the full antenna of UTR-2 includes twelve identical sections, but for solar observations a part of them is quite enough. The total effective area of these four sections is about 50,000 m^2 with a beam pattern size of $1^\circ \times 15^\circ$ at 25 MHz. Figure 1 shows the dynamic radio spectrum for one of the many events with a high-frequency cut-off, received with the telescope. The data were recorded by the digital DSP spectrometer [Ryabov et al., 2010] operating in the frequency range of 9–33 MHz with a frequency–time resolution of 4 kHz and 100 ms, respectively.

By a special adaptive procedure the contribution of radio frequency interferences (RFI), contaminating the spectrum, was reduced significantly. The procedure consisted of several stages. Firstly, we determined iteratively the mean and standard deviation (σ) in each frequency channel, clipping the signal values above 3σ at each channel, but this procedure reduces only the strongest RFIs (outliers). Often the presence of outliers has a strong effect on the mean and the standard deviation, making this technique less reliable. Since the median is less sensitive to outliers than the mean, the Median Absolute Deviation (MAD) can be used as the variance estimator [Leys et al., 2013]. Then each sample of the observation record is modified by the absolute value of the median subtracted from

Table 1: Activity overview of 18 August 2012 from UTR-2 radio observations, http://www.swpc.noaa.gov/ and http://cdaw.gsfc.nasa.gov/. The time interval of available UTR-2 spectral data was 06:00–12:00 UT.

#	Activity	Features	Start Time
1	Flares	GOES class M5.5, NOAA active region 11548	00:24 UT
		GOES class M1.8, NOAA active region 11548	03:17 UT
		GOES class C6.1, NOAA active region 11548	06:09 UT
		GOES class C2.6, NOAA active region 11548	08:30 UT
		GOES class C1.9, —	08:50 UT
		GOES class C1.0, NOAA active region 11548	09:46 UT
		GOES class C1.9, NOAA active region 11548	10:32 UT
		GOES class C1.3, NOAA active region 11548	11:41 UT
		GOES class C2.4, —	11:49 UT
		GOES class C1.0, —	12:23 UT
		GOES class C2.1, NOAA active region 11548	13:29 UT
		GOES class C7.3, NOAA active region 11548	14:18 UT
		GOES class C1.3, NOAA active region 11548	14:58 UT
		GOES class M2.0, NOAA active region 11548	16:02 UT
		GOES class C2.5, NOAA active region 11548	19:06 UT
		GOES class C1.1, NOAA active region 11548	21:20 UT
		GOES class M1.0, NOAA active region 11548	22:46 UT
		GOES class M1.3, NOAA active region 11548	23:15 UT
2	CMEs	partial halo, bright eruption	00:48 UT
		partial halo, narrow eruption	03:36 UT
			05:12 UT
		narrow eruption	06:12 UT
			08:48 UT
			09:48 UT
		faint eruption	10:12 UT
			10:48 UT
			11:24 UT
			12:36 UT
		narrow eruption	13:26 UT
			14:48 UT
		partial halo, narrow eruption	16:24 UT
			17:36 UT
			19:48 UT
			21:12 UT
		bright narrow eruption	23:36 UT
3	Radio events	type III and IIIb–III bursts as well as solar bursts with high-frequency cut-off	

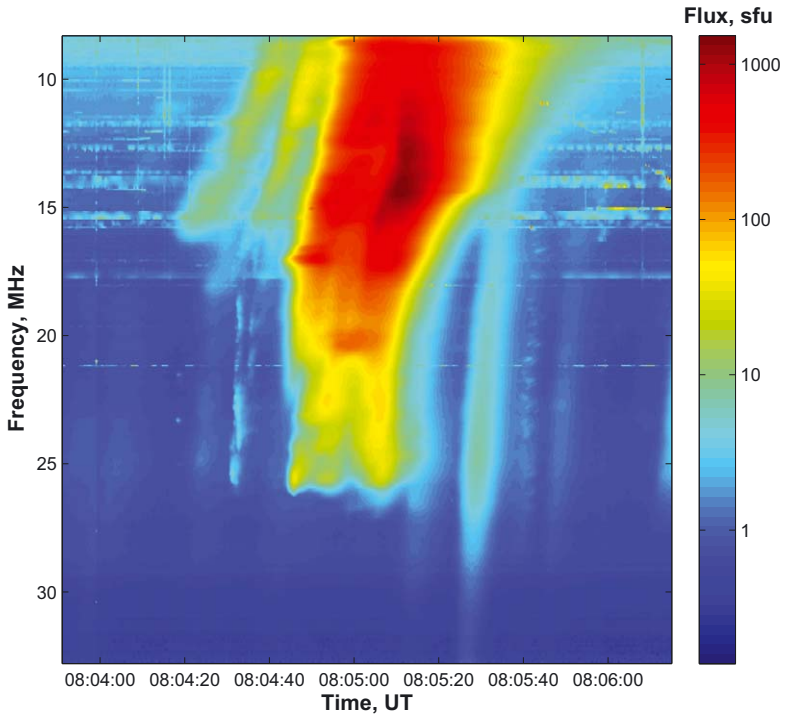

Figure 1: One of the behind–limb bursts observed on 18 August 2012 at decameter wavelengths by the UTR-2 radio spectrograph.

each sample, i. e.

$$\mathrm{MAD} = b\, M_i(|x_i - M_j(x_j)|)\,,$$

where x_j denotes the n original observation samples, and M_i is the median of the series. Usually a constant $b = 1.4826$ is assumed from the normality of the data. Next, the threshold level χ is calculated for each frequency channel as $\chi_i = M(x_i) - \beta\,\mathrm{MAD}$ with the aggressiveness parameter β (its value is 2.5). This allows us to get a flag mask with the "bad" (interference) samples. In the final stage we interpolated and extrapolated holes in the frequency–time data array.

An unusual set of solar bursts was observed from 17 August to 19 August 2012 with different cut-off frequencies. The maximum radio flux of the events was about $10^2 - 10^3$ s.f.u. (1 s.f.u = 10^{-22} W m^{-2} Hz^{-1}). Several features of the bursts on 18 August 2012 are shown in Table 2. Their degree of polarization was lower (∼10–15%), as if the bursts were emitted at the second harmonic of the local plasma frequency [Brazhenko et al., 2015]. The polarization measurements were carried out by the radio telescope URAN-2 (near Poltava, Ukraine). Although the frequency drift rate of the bursts is atypical for both type II and type III bursts, this does not mean that the bursts belong to a new type of solar bursts. Likely, the peculiarity can be connected with the origin of the cut-off occurrence [Stanislavsky et al., 2016]. Moreover, on 19 August 2012 at ∼11:23 UT UTR-2 has received a group of solar bursts with high-frequency cut-off, having frequency drift rates and durations typical for the type III solar bursts in the decameter wavelengths range [Stanislavsky, 2017]. Note that the range of cut-off frequencies was

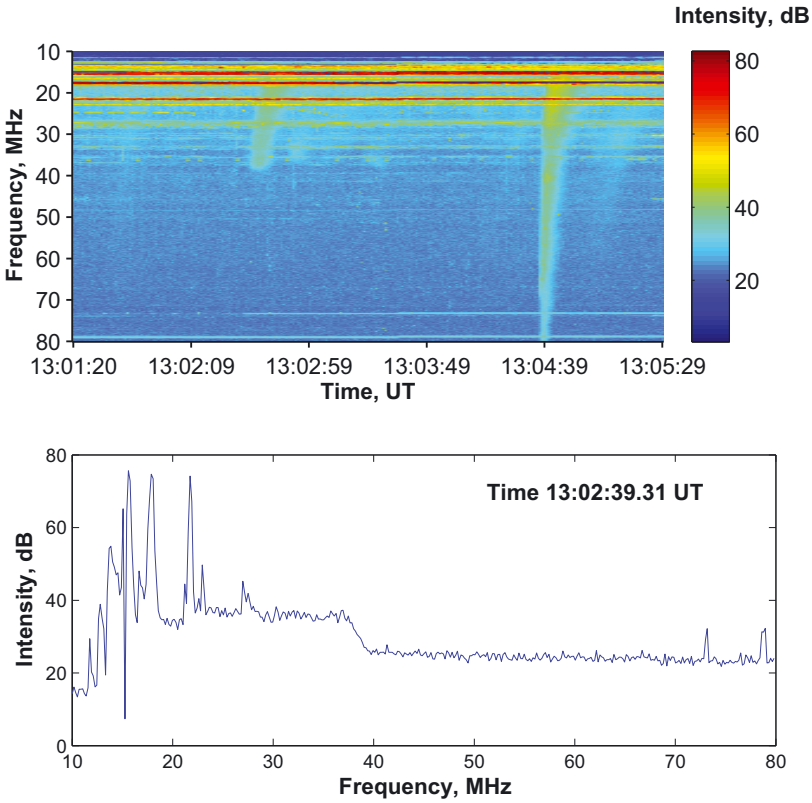

Figure 2: Example of a burst with high-frequency cut-off received by the Nançay Decametric Array. The top picture shows two solar bursts on 18 August 2012: the left one has cut-off at 40 MHz, whereas the right one was ordinary. The bottom plot is a profile of the left solar burst.

about 10–70 MHz, and a part of the observed bursts possessed a cut-off frequency out of the frequency range of the UTR-2 facilities. To avoid this restriction, we took into account the solar radio data recorded by other radio telescopes. In particular, the Nançay Decametric Array (NDA) performed appropriate observations on 17–19 August 2012. The radio telescope has 2×72 helical spiral antennae working at 10–80 MHz [Boischot et al., 1980]. Unfortunately, the NDA sensitivity is weak below 30 MHz, and the radio ambiance contains a lot of strong low-frequency natural and artificial disturbances. Nevertheless, the radio tool demonstrates acceptable performance above 30 MHz. We make use of the solar NDA data which is freely available (see `http://bass2000.obspm.fr/home.php`). Figure 2 represents one of the dynamic radio spectra, where two similar solar bursts were seen, but only one had a high-frequency cut-off whereas the other did not. Their features look like those of type III solar bursts. Table 3 collects properties of the solar bursts with cut-off frequencies higher than the ones observed by UTR-2 (see, for comparison, Table 2). In both tables the cut-off in the dynamic spectra of any burst is determined by two frequencies: the start point and the end frequency between which the burst intensity drops to the background level (pedestal) of radio emission at which the corona radiates only as a thermal source. Below we are going to estimate a source size of the solar bursts, using the values of the cut-off frequencies.

Table 2: Properties of the solar bursts with high-frequency cut-off from 18 August 2012 from the UTR-2 radio observations.

Time, UT	Frequency drift rate, [MHz/s]	Start frequency of cut-off, [MHz]	End frequency of cut-off, [MHz]
06:39	0.35±0.05	20.9±0.1	18.2±0.1
07:10	0.6±0.05	19.4±0.1	14.5±0.1
08:04	0.53±0.05	27.4±0.1	23.4±0.1
08:15	0.67±0.05	19.4±0.1	15.1±0.1
09:05	0.5±0.05	20.7±0.1	17.6±0.1
11:06	0.33±0.05	15.6±0.1	11.7±0.1
11:35	2.17±0.05	26.±0.1	22.9±0.1
11:37	0.57±0.05	19.9±0.1	17.9±0.1
11:55	0.5±0.05	12.4±0.1	10.6±0.1

Table 3: Properties of the solar bursts with high-frequency cut-off from 18 August 2012 from the NDA radio observations.

Time, UT	Frequency drift rate, [MHz/s]	Start frequency of cut-off, [MHz]	End frequency of cut-off, [MHz]
10:36	6.8±0.2	45±0.5	43±0.5
11:49	4.8±0.2	65±0.5	61±0.5
13:03	2.5±0.2	40±0.5	37±0.5
13:18	5.3±0.2	66±0.5	60±0.5
13:34	2.8±0.2	38±0.5	33±0.5
13:36	2.1±0.2	43±0.5	37±0.5
13:37	2.1±0.2	43±0.5	37±0.5
14:25	2.7±0.2	43±0.5	36±0.5

The high-frequency cut-off can be explained as a propagation effect between the source and the observer [Melnik et al., 2014; Stanislavsky et al., 2016]. In this case the radiating source arises behind the Sun relative to an observer on Earth. Moving radially, its radiation is reflected away from Earth because the solar corona is opaque to radio emission with frequencies below the local plasma frequency. This resembles something like the occultation in which a star (and its radio emission) is covered, for example, by the Moon's limb. The behind–limb burst emission appears for terrestrial observers when the electron density (decreasing with height) in the solar corona allows the radio emission to pass towards Earth. Recall here that the method of lunar occultation is applied for many problems: determining the diameters of asteroids, planets and stars, discovering and examining close binary stars and even studying the distribution of brightness on the disks of some stars [see, for example, Fors et al., 2001; Bergeat et al., 2001; Jatmiko et

al., 2014 and references therein]. Today this approach remains one of the most sensitive methods to measure the angular size of radio sources.

3 Radio occultation of burst sources by the solar corona

In the Rayleigh–Jeans limit the brightness temperature T_b of a source region of radio emission depends on two values: the flux F (the power per unit frequency interval that passes through a surface of unit area) and the solid angle Θ, defining the fraction of the entire sky which is covered by the source, the whole sky having a solid angle of 4π. For a small circular source, the solid angle is computed [Kraus, 1967] as $\Theta = \theta_s^2\pi/4$, where θ_s is the angular diameter of the radio source under consideration. Then the brightness temperature of its radio emission satisfies the formula $T_b = F\lambda^2/(2k\Theta)$, depending on the wavelength λ. Here $k = 1.38 \times 10^{-23}$ J/K denotes Boltzmann's constant. In our observations by means of UTR-2 the dynamic spectra of solar bursts have been already obtained in solar flux units (see Figure 2). To get a frequency–time representation of solar bursts in brightness temperature, we have to determine their angular size.

The high-frequency cut-off in solar bursts is somewhat similar to an occultation effect with the difference that its origin is caused by the solar corona rather than by the Moon. In the broadest sense, the term "occultation" refers to the complete or partial obscuring of an astronomical object by another. Recall also, the occultation of cosmic radio sources (for example, Taurus A or Crab Nebula) by the solar corona has been studied over many years [Vitkevich, 1951; Machin and Smith, 1952; Slee, 1959]. Both angular and spectral broadening of spacecraft radio signals were observed independently during coronal occultation too [Bradford and Routledge, 1980; Bird, 1982]. Using the solar eclipse on 15 January of 2010 to study the solar corona at low radio frequencies, Ramesh et al. [2012] found the angular size of the smallest source observable at 109–150 MHz. Just like for the lunar occultation of radio sources, the limiting resolution is given by the width θ of the first zone of the Fresnel diffraction pattern in the form of $\theta = \sqrt{0.5\lambda/D_M}$, where λ denotes the wavelength of observation, and D_M is equal to the Earth–Moon distance ($\approx 3.8 \times 10^8$ m). The radio occultation of low-frequency burst sources by the solar corona is characterized by a similar relation, namely $\theta = \sqrt{0.5\lambda/D_S}$, where D_S is the Earth–Sun distance ($\approx 1.5 \times 10^{11}$ m). Notice that in the latter case the angular resolution of the interferometer is about 20 times more than for the lunar occultation. If the high-frequency cut-off in the events on 17–19 August of 2012 is a result of the radio occultation of their solar burst sources due to the solar corona, then we can estimate their angular sizes from the cut-off frequencies. The important advantage of this approach is that it enables to determine the source size independently from the size of the radio antenna aperture used in observations.

From the study of radio profiles with cut-off it is clear that any diffraction effect is lacking. Thus, the difference of frequencies between the start point (f_1) and the end one (f_2), where the bursts (because of the cut-off) fall to a background level of radio emission in intensity, is just defined by the angular size of corresponding sources in the given height of the corona. If we know the values r_1 and r_2 for the frequencies f_1 and f_2, respectively (using the relation $f[\mathrm{MHz}] \approx 9000\sqrt{n_e}\,[\mathrm{cm}^{-3}]$ and the electron density $n_e(r)$ of the solar

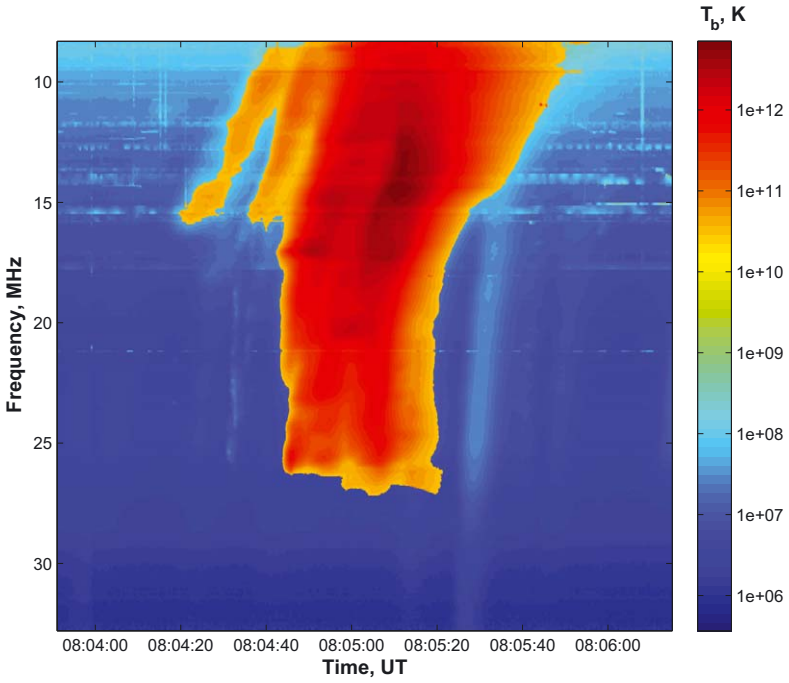

Figure 3: Dynamic spectrum of the solar burst (18 August 2012) with high-frequency cut-off in brightness temperature. The electron density model was taken in the Baumbach–Allen's form.

corona in dependence on the height r), then the angular size of the moving source may be estimated as $\theta_s \approx |r_1 - r_2|/D_S$. Unfortunately, the knowledge about the electron density of the solar corona has a semi–empirical character. There exists a set of different models, describing the density fall-off with height of the equatorial quiet corona, active regions, coronal holes and so on [see Allen, 1947; Newkirk, 1961; Mann et al., 1999]. The choice of the model affects both the resulting height r and the derived angular size θ_s. A much better result would be gained by utilizing actual density measurements of the corona in required places, but this is hardly possible to perform in the common case. Therefore, we considered three popular (so-called Newkirk's, Baumbach–Allen's and Mann's) models of coronal density and compared their contribution. Another important point is that each burst with a high-frequency cut-off gives one angular source size, only corresponding to its cut-off frequency. Usually the source size of solar bursts increases with decreasing frequency as it is well known, for example, in the type III bursts, see e.g. Reid and Ratcliffe [2014]. By our procedure we will find an "averaged" evolution of source sizes in frequency, using the cut-off frequencies of the solar bursts mentioned in Tables 2 and 3.

The source size evolution in frequency can be explained by the decollimation of electron beams, generating the solar bursts, by inhomogeneities in the solar corona. Due to the measurements of source sizes at different frequencies for type III bursts, the average values are equal to 28–30 arcmin at 26.4 MHz [Chen and Shawhan, 1978], 20 arcmin at 43 MHz, 11 arcmin at 80 MHz and 5 arcmin at 169 MHz [Dulk and Suzuki, 1980], 4.5 arcmin at 150 MHz and 2 arcmin at 432 MHz [Saint–Hilaire et al., 2013]. Then the source widths are fitted by the power–law relation $\theta(\text{arcmin}) \approx 659.4/f^{0.97}$, where f is the frequency in MHz.

It is interesting that the comprehensive study of type III radio source sizes at frequencies below 2 MHz also indicates a frequency dependence of source angular size close to f^{-1} [Steinberg et al., 1985]. Following the Newkirk's, Baumbach–Allen's and Mann's models of coronal density, the average angular source sizes of behind–limb bursts are given by the relations $\theta_{\rm N}(\text{arcmin}) \approx 157.8/f^{1.4}$, $\theta_{\rm BA}(\text{arcmin}) \approx 13.1/f^{1.02}$ and $\theta_{\rm M}(\text{arcmin}) \approx 53.7/f^{1.18}$, respectively. Notice that the Baumbach–Allen's model is the best giving a f^{-1} variation of source angular size with observing frequency. However, there is a significant difference in the average source sizes of the behind–limb bursts and ordinary type III bursts. This can be explained in terms of the reduced number of inhomogeneities in the solar corona for a given direction due to accompanied CMEs, and/or this is a result of focusing the solar bursts on low–density cavities in the CMEs. Why can the behind–limb bursts be similar to the type III ones? Firstly, the type III bursts are the most numerous events in solar activity. On the other hand, there is a real confirmation in our radio data recorded on 19 August 2012. There was a group of solar bursts with high-frequency cut-offs that had frequency drift rates and durations of individual bursts typical for type III radio bursts at low frequencies [Stanislavsky, 2017].

Estimating the average source size variation of solar bursts with a high-frequency cut-off, we have found the brightness temperature T_b of the radio source for the behind–limb burst shown in Figure 2. Consequently, its dynamic spectrum in brightness temperature is represented in Figure 3. In the given frequency range the greatest brightness temperature of this burst reached about 7.1×10^{12} K which corresponds to brightness temperatures of type III solar bursts in moderate intensity. Note that this burst is imposed on a background (thermal radio emission) with a brightness temperature of about 10^6 K. Other bursts given in Table 2 show approximately similar values of maximum brightness temperatures, 10^{12}–10^{13} K. Unfortunately, the bursts of Table 3 were not calibrated in flux.

4 Conclusions

We have analyzed features of solar bursts with high-frequency cut-offs observed on 17–19 August 2012. The largest number of such bursts were recorded on 18 August, and we have paid the most attention to the data of this day. In this experiment, to achieve the best reliability of obtained data, the different ground-based observatories, located at significant distances from each other, were involved, but the Ukrainian radio telescope UTR-2 has played a crucial role. Now, with full confidence we can affirm that the high-frequency cut-off arises exactly in solar corona. The cut-off effect is explained by the generation of the bursts behind the solar limb with respect to observers on Earth. Using the cut-off frequencies from the study of different bursts, we have estimated the average source size development of behind–limb bursts in frequency. As our measured dynamic spectra were in solar flux units, the knowledge about angular sizes of burst sources allowed us to establish their brightness temperature. There is reason to believe that the solar bursts with high-frequency cut-offs are nothing else but type III radio bursts. Their fine structure can be explained by the peculiarity of radio wave propagation out of limb zones.

Acknowledgments. We want to thank the GOES, STEREO, SOHO and NDA teams for developing and operating the instruments as well as for their open data policy. The

authors are grateful to the Nançay team for free access of the NDA data (`https://realtime.obs-nancay.fr/`). This research was also partially supported by Research Grants 0115U004085, 0117U002395 from the National Academy of Sciences of the Ukraine. The authors are grateful to I. Y. Vasylieva and V. A. Shepelev for their remarks and useful discussions. The authors thank the anonymous referees for valuable comments on the manuscript. The Editors also thank two anonymous referees for their help in evaluating this paper.

References

Allen, C. W., Solar radio–noise of 200 Mc./s. and its relation to solar observations, *Mon. Not. Roy. Astron. Soc.*, **107**, 386–396, 1947.

Bergeat, J., A. Knapik, and B. Rutily, The effective temperatures of carbon–rich stars, *Astron. Astrophys.*, **369**, 178–209, 2001.

Bird, M. K., Coronal investigations with occulted spacecraft signals, *Space Sci. Rev.*, **33**, 99–126, 1982.

Boischot, A., C. Rosolen, M. G. Aubier, G. Daigne, F. Genova, Y. Leblanc, A. Lecacheux, J. de la Noë, and B. Møller–Pedersen, A new high–gain, broadband, steerable array to study Jovian decametric emission, *Icarus*, **43**, 399–407, 1980.

Bradford, H. M., and D. Routledge, Coronal occultation of Voyager 2, 1979 August, *Mon. Not. Roy. Astron. Soc.*, **190**, 73P–77P, 1980.

Braude, S. Ya., A. V. Megn, B. P. Ryabov, N. K. Sharykin, and I. N. Zhouck, Decametric survey of discrete sources in the northern sky. I – The UTR-2 radio telescope: Experimental techniques and data processing, *Astrophys. Space Sci.*, **54**, 3–36, 1978.

Brazhenko, A. I., V. N. Melnik, A. V. Frantzusenko, H. O. Rucker, and M. Panchenko, Unusual solar decameter radio bursts with high-frequency cut-off (in Russian), *Radio Phys. and Radio Astron.*, **20**, 10–19, 2015.

Chen, H. S.–L., and S. D. Shawhan, Structure and evolution of solar radio bursts at 26.4 MHz, *Solar Phys.*, **57**, 205–227, 1978.

Dulk, G. A., and S. Suzuki, The position and polarization of type III solar bursts, *Astron. Astrophys.*, **88**, 203–217, 1980.

Fors, O., J. Núñez, and A. Richichi, CCD drift–scan imaging lunar occultations: A feasible approach for sub-meter class telescopes, *Astron. Astrophys.*, **378**, 1100–1106, 2001.

Jatmiko, A. T. P., G. P. Puannandra, R. D. Hapsari, R. A. Putri, Z. M. Arifin, G. K. Haans, and I. P. W. Hadiputrawan, Lunar occultation observation of μ Sgr: A progress report, in *AIP Conference Proceedings*, **1589**, 53–56, 2014.

Kraus, J. D., Radio Astronomy, McGraw–Hill Book Company, New York, USA, 1967.

Konovalenko, A. A., et al. (71 co-authors), The modern astronomy network in Ukraine: UTR-2, URAN and GURT, *Exp. Astron.*, **42**, 11–48, 2016.

Leys, C., C. Ley, O. Klein, P. Bernard, and L. Licata, Detecting outliers: Do not use standard deviation around the mean, use absolute deviation around the median, *J. Exper. Soc. Psych.*, **49**, 764–766, 2013.

Machin, K. E., and F. G. Smith, Occultation of a radio star by the solar corona, *Nature*, **170**, 319–320, 1952.

Mann, G., F. Jansen, R. J. MacDowall, M. L. Kaiser, and R. G. Stone, A heliospheric density model and type III radio bursts, *Astron. Astrophys.*, **348**, 614–620, 1999.

Melnik, V. N., A. I. Brazhenko, A. A. Konovalenko, H. O. Rucker, A. V. Frantsuzenko, V. V. Dorovskyy, M. Panchenko, and A. A. Stanislavsky, Unusual solar radio burst observed at decameter wavelengths, *Solar Phys.*, **289**, 263–278, 2014.

Newkirk, G. Jr., The solar corona in active regions and the thermal origin of the slowly varying component of solar radio radiation, *Astrophys. J.*, **133**, 983–1013, 1961.

Ramesh, R., C. Kathiravan, I. V. Barve, and M. Rajalingam, High angular resolution radio observations of a coronal mass ejection source region at low frequencies during a solar eclipse, *Astrophys. J.*, **744**, id.165, 2012.

Ryabov, V. B., D. M. Vavriv, P. Zarka, B. P. Ryabov, R. Kozhin, V. V. Vinogradov, and L. Denis, A low–noise, high dynamic range digital receiver for radio astronomy applications: An efficient solution for observing radio–bursts from Jupiter, the Sun, pulsars and other astrophysical plasmas below 30 MHz, *Astron. Astrophys.*, **510**, id.A16, 2010.

Reid, H. A. S., and H. Ratcliffe, A review of solar type III radio bursts, *Res. Astron. Astrophys.*, **14**, 773–804, 2014.

Saint–Hilaire, P., N. Vilmer, and A. Kerdraon, A decade of solar type III radio bursts observed by the Nançay radioheliograph 1998–2008, *Astrophys. J.*, **762**, id.60, 2013.

Slee, O. B., Occultations of the Crab nebula by the solar corona in June 1957 and 1958, *Austr. J. Phys.*, **12**, 134–156, 1959.

Stanislavsky, A. A., A. A. Konovalenko, A. A. Koval, Ya. S. Volvach, and P. Zarka, CMEs and frequency cutoff of solar bursts, *Sun and Geosphere*, **11**, 2, 91–95, 2016.

Stanislavsky, A. A., Solar type III bursts with high-frequency cut-off, *Astronom. Nachr.*, **338**, 407–412, 2017.

Steinberg, J. L., S. Hoang, and G. A. Dulk, Evidence of scattering effects on the sizes of interplanetary type III radio bursts, *Astron. Astrophys.*, **150**, 205–216, 1985.

Vitkevich, V. V., New method for studying the solar corona, *Dokl. Akad. Nauk SSSR*, **77**, 585–593, 1951.